RC23513 (W0502-039) February 4, 2005
Materials Science

IBM Research Report

Effect of Intermetallics Spalling on the Mechanical Behavior of Electroless Ni(P)/Pb-free Solder Interconnection

Yoon-Chul Sohn, Jin Yu
KAIST
373-1, Guseong-Dong, Yuseong-Gu
Daejeon 305-701
Korea

Sung K. Kang, Da-Yuan Shih
IBM Research Division
Thomas J. Watson Research Center
P.O. Box 218
Yorktown Heights, NY 10598

Taek-Yeong Lee
Hanbat National University
San 16-1, Dukmyoung-Dong, Yuseong-Gu
Daejeon
Korea

Research Division
Almaden - Austin - Beijing - Haifa - India - T. J. Watson - Tokyo - Zurich

Effect of Intermetallics Spalling on the Mechanical Behavior of Electroless Ni(P)/Pb-free Solder Interconnection

Yoon-Chul Sohn, Jin Yu, Sung K. Kang*, Da-Yuan Shih* and Taek-Yeong Lee**
Dept. of Mater. Sci. Eng., KAIST, 373-1, Guseong-Dong, Yuseong-Gu, Daejeon 305-701, Korea
*IBM T. J. Watson Research Center, 1101 Kitchawan Rd., Rt. 134, Yorktown Heights, NY 10598, USA
**Dept. of Mater. Eng., Hanbat National University, San 16-1, Dukmyoung-Dong, Yuseong-Gu, Daejeon, Korea
sonyc@kaist.ac.kr, Tel. 82-42-869-4274, Fax. 82-42-869-8840

Abstract

A systematic investigation of mechanical testing was conducted to correlate the brittle fracture observed in Ni(P) metallization with Ni-Sn intermetallic spalling in Pb-free solder joints. To produce lap shear test samples, two FR4 PCBs finished with Ni(P)/Au were reflowed using two Pb-free solders, Sn-3.5Ag and Sn-3.0Ag-0.5Cu (in wt.%). Brittle fracture was found in the solder joints made of Sn-3.5Ag, while only ductile fracture was observed in the Cu-containing solder (Sn-3.0Ag-0.5Cu). For Sn-3.0Ag-0.5Cu joints, $(Ni,Cu)_3Sn_4$ and/or $(Cu,Ni)_6Sn_5$ IMCs were formed at the interface between the solder and Ni(P) film. For Sn-3.5Ag, Ni_3Sn_4 was formed and spalled off the Ni(P) film, causing brittle fracture in solder pads where Ni_3Sn_4 had spalled. From the analysis of fracture surfaces, it was found that the brittle fracture occurs through the Ni_3SnP layer The growth of the Ni_3SnP layer appears to be responsible for Ni_3Sn_4 spalling and thereby for the brittle fracture of Ni(P)/solder interconnection.

To prevent IMC spalling from the Ni(P) metallization, a thin intermediate layer of Sn or Cu was deposited by electrolytic or electroless plating method on the Ni(P) film. During the reflow reaction of Sn-3.5Ag solder paste, the intermediate layers effectively suppressed Ni_3Sn_4 spalling during the reflow reaction at 250°C for 30 min, while Ni_3Sn_4 easily spalled off the Ni(P) film in a few minutes in the control samples without an intermediate layer.

Introduction

Electroless Ni(P)/immersion gold (ENIG) has been used for under bump metallization (UBM) of flip chip and ball grid array (BGA) and as a surface finish layer of printed circuit boards (PCB).[1-9] Electroless Ni(P) is selectively deposited on metal surfaces with a uniform thickness.[10,11] Immersion gold layer prevents the Ni(P) layer from oxidation and enhances wettability of solders.[7] However, the Ni(P) metallization has two technical concerns against extensive commercial application. The first one is spalling of intermetallic compound (IMC) during the wetting reaction with Sn-containing solders.[9,12] IMC spalling from other thin film UBMs has been found only after a complete consumption of the film. The Ni(P) metallization, however, shows the spalling phenomena before consuming all of the metallization. The second concern is brittle fracture phenomena,[1-8] reported in surface mount BGA packages on a printed circuit board (PCB) with ENIG metallization on the pads. The failure has been reported to be unpredictable and occur at relatively low defect levels.[5] Interfacial P segregation [2], void and crack formation during the crystallization of the Ni(P) film into Ni_3P phase [7], or hyperactive corrosion of the Ni(P) film during the immersion gold plating [3] have been suggested as possible causes of the brittle fracture. The mechanism of the brittle fracture, however, has not been well understood yet. In this study, the relationship between IMC spalling and the brittle fracture of ENIG/solder interconnection was systematically investigated. In addition, a method to prevent IMC spalling and thereby to reduce the brittle fracture was demonstrated by deposition of a thin ntermediate layer of Sn or Cu on top of the Ni(P) film.

Experimental

A specimen for lap-shear testing is composed of two FR4 PCBs having 16 solder pads with 250μm diameter. The PCB size was 10×10 mm^2 and 10×30 mm^2 for the top and bottom substrate, respectively. The same UBM, Cu/Ni(7P)/Au, was used for both sides. Ni(7P) means that the film has 7wt.% P. The schematic diagrams of the test specimen and metallization scheme are presented in Fig. 1(a) and (b). Sn-3.5Ag or Sn-3.0Ag-0.5Cu (all in wt.% unless specified otherwise) solder paste was deposited on the bottom PCB and reflowed for 1min at 250°C in N_2 atmosphere. Then, the top PCB was joined by the second reflow for 1 or 5min at 250°C. Shear testing was conducted at a loading rate of 0.2mm/min with the specimen held in a stainless steel jig as depicted in Fig. 1(a).

Intermediate layers to prevent the spalling were deposited on the Ni(9P) film with commercial electrolytic or electroless plating solutions. A substrate for this reaction study was a Si wafer on which Cr/Cu thin films had been consecutively sputtered. A schematic structure is presented in Fig. 1(c). Electroless Cu was plated about 0.7μm thick at 33°C ± 1°C with a solution from C. Uyemura Co., Ltd. Soldering was performed using Sn-3.5Ag solder paste at 250°C up to 30min. The solder joints were investigated using scanning electron microscopy (SEM) with energy dispersive x-ray spectroscopy (EDX). Cross-sectional SEM specimens were prepared by the standard procedure of epoxy-mounting, polishing and selective etching.

Results and Discussion

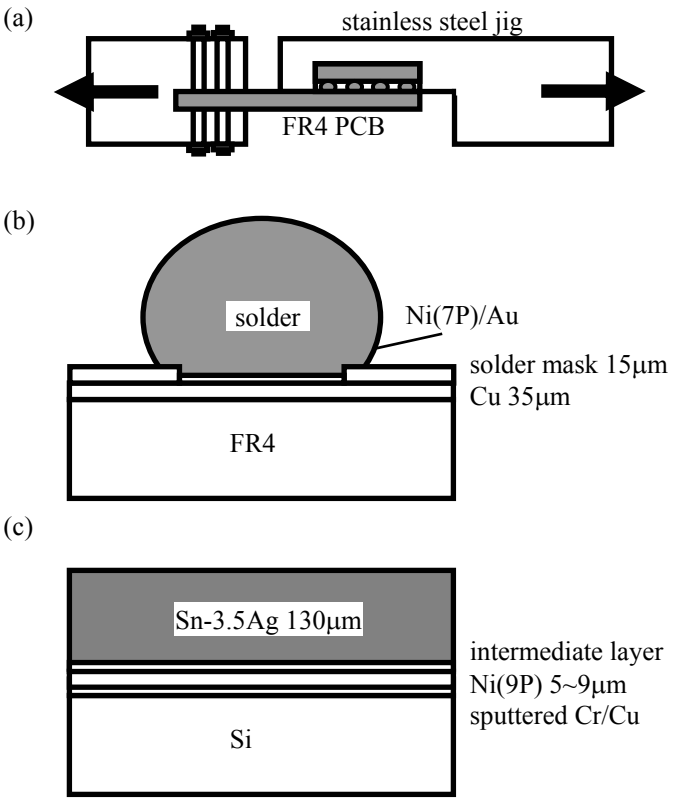

Fig. 1. Schematic diagrams showing (a) a shear-test specimen held in stainless steel jig, (b) a solder pad in the shear-test specimen, and (c) a specimen for the reaction study with intermediate layers.

1) Interfacial reactions

After the 1st reflow to the bottom PCB, needle-like Ni_3Sn_4 IMC was formed with some chunks at Sn-3.5Ag solder joint, while layer-type $(Cu,Ni)_6Sn_5$ formed at Sn-3.0Ag-0.5Cu joint as shown in Fig. 2(a) and (b). For the Sn-3.5Ag joint, the spalling of Ni_3Sn_4 IMC increased as reflow time increased as shown in Fig. 2(c) and (e). In case of Sn-3.0Ag-0.5Cu, $(Ni,Cu)_3Sn_4$ IMC was formed at top joints instead of the $(Cu,Ni)_6Sn_5$ IMC as Cu concentration in the solder deceased due to the formation of $(Cu,Ni)_6Sn_5$ during the 1st reflow. For an extended reflow time such as 6 min, at bottom joints, $(Ni,Cu)_3Sn_4$ IMC grew underneath the $(Cu,Ni)_6Sn_5$ IMC, which was finally separated from the $(Ni,Cu)_3Sn_4$,as shown in Fig. 2(f).

It was reported that Ni_3Sn_4 IMC was formed on Ni UBM during the reaction with Sn-3.5Ag and $(Cu,Ni)_6Sn_5$ ternary IMC with Sn-3.5Ag-0.5Cu. [13] The growth rate of $(Cu,Ni)_6Sn_5$ was faster than Ni_3Sn_4. It was also pointed out that $(Ni,Cu)_3Sn_4$ IMC grew underneath the $(Cu,Ni)_6Sn_5$ IMC when the Cu content in the solder decreased to 0.2 wt.%. However, in the present study, we observed that Ni_3Sn_4 in Sn-3.5Ag grew thicker than the Ni-Cu-Sn ternary IMCs, $(Cu,Ni)_6Sn_5$ or $(Ni,Cu)_3Sn_4$, in Sn-3.5Ag-0.5Cu as shown in Fig. 2. In addition, Ni_3Sn_4 IMC spalled, while the ternary IMCs didn't spalled off the Ni(P) surface. The spalling behavior was closely related with IMC morphology and crystallization of the Ni(P) film. Ni3Sn4 on the Ni(P) metallization initially

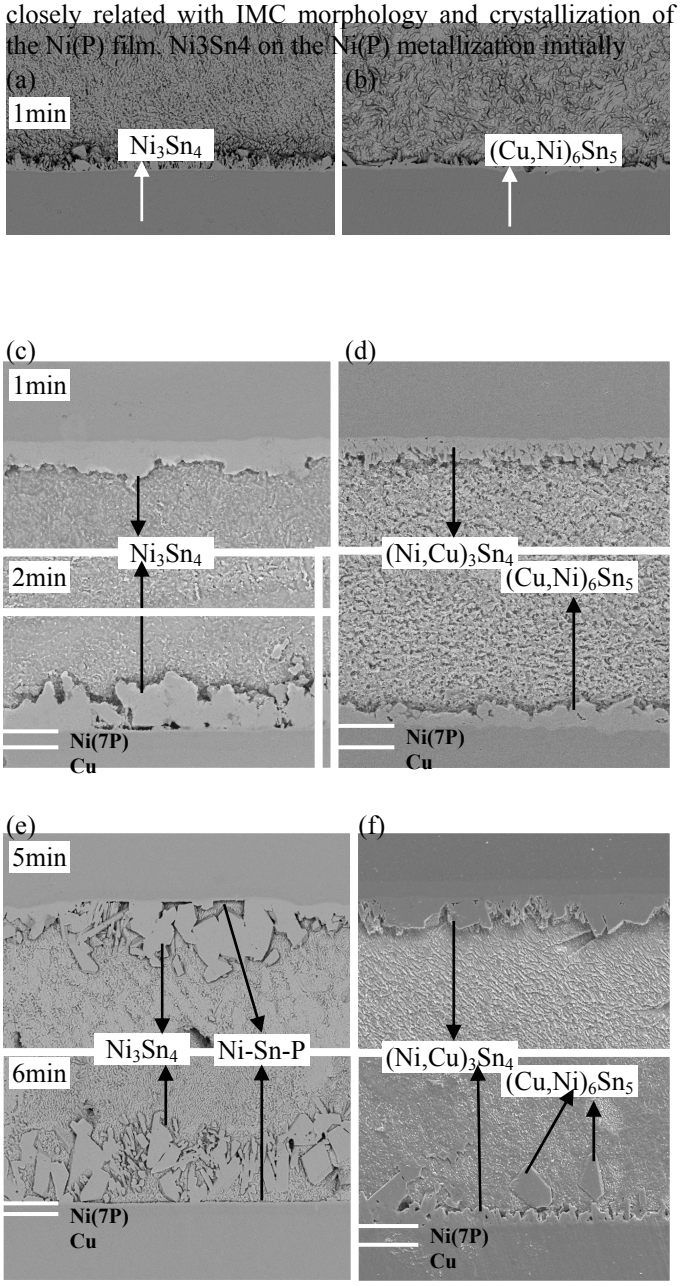

Fig. 2. Cross-sectional micrographs showing bottom joint after the 1st reflow (a) with Sn-3.5Ag and (b) with Sn-3.0Ag-0.5Cu, top and bottom joint after the 2nd 1min reflow (c) with Sn-3.5Ag and (d) with Sn-3.0Ag-0.5Cu, and after the 2nd 5min reflow (e) with Sn-3.5Ag and (f) with Sn-3.0Ag-0.5Cu (all the pictures are in same magnification).

grew with needle-like morphology [12], while the ternary IMCs was formed as a layer-type. The layer-type IMCs effectively reduce the interaction between solder and the Ni(P) film as good diffusion barriers. [9,14] However, molten Sn can easily reach the interface between Ni_3Sn_4 and the Ni(P) film through many channels among needle-like Ni_3Sn_4 IMCs.

A part of the Ni(P) film underneath the Ni_3Sn_4 IMC crystallized into a Ni_3P phase due to Ni out-diffusion and P enrichment in the region. [15,16] Also, a thin nanocrystalline Ni-Sn-P layer was found on top of the Ni_3P layer, confirmed as

Ni_3SnP phase by TEM investigations. [12,17,18] In the previous study [12], we pointed out that growth of the Ni_3SnP layer caused Ni_3Sn_4 spalling and that Ni consumption and crystallization of the Ni(P) film were accelerated after the spalling. The Ni_3SnP layer kept growing after the spalling. As a result, after the same reaction time, the thickness of remaining Ni(P) film was smaller in Sn-3.5Ag than in Sn-3.0Ag-0.5Cu solder as shown in Fig 2(e) and (f). A thin Au layer on the Ni(P) film is known to be quickly dissolved in a solder and not to participate in the interfacial reaction. [17,18]

During the reaction between Ni and Sn-3.9Ag-xCu, Ho et al. reported a formation of $(Cu,Ni)_6Sn_5$ IMC if $x \geq 0.5$, and $(Ni,Cu)_3Sn_4$ if $x \leq 0.4$. [19,20] In this study, the thickness of $(Cu,Ni)_6Sn_5$ IMC formed in Sn-3.0Ag-0.5Cu was measured to be 1.61(±0.43)μm at the bottom joint after the 1st reflow. During the 2nd 1min reflow, the $(Cu,Ni)_6Sn_5$ IMC grew up to 3.04(±0.57)μm while $(Ni,Cu)_3Sn_4$ grew to 3.38(±0.58)μm thick at the top joint. After 6min reflow, $(Cu,Ni)_6Sn_5$ was detached as $(Ni,Cu)_3Sn_4$ grew underneath the $(Cu,Ni)_6Sn_5$ IMC as shown in Fig. 2(f). The type and spalling behavior of the IMCs are summarized in Table Ⅰ.

Using the IMC thickness data measured, the Cu concentration or number of remaining Cu atoms in the solder after a reflow reaction can be estimated from the following equation (1).

$$N_{Cu} = \frac{V_s \rho_s N_A n}{M_{Cu}} - \frac{A t_I \rho_I N_A m}{M_I} p \qquad (1)$$

where subscript s and I represent solder and IMC. (V, ρ, M ; volume, density, molecular(atomic) mass, N_A ; Avogadro's number, n ; wt.% of Cu in the solder before reaction, A ; area of the solder pad, t ; thickness of IMC, m ; number of Cu (Ni) atoms per a molecule of IMC, and p ; fraction of Cu occupying Cu (Ni) sites of the IMC lattice) For the calculation, we assumed that densities of $(Cu,Ni)_6Sn_5$ and $(Ni,Cu)_3Sn_4$ are the same as Cu_6Sn_5 (8.28g/cc) and Ni_3Sn_4(8.65g/cc). [21] p was set as 0.6 and 0.2 for the former and latter IMC based on EDX analysis and literatures ; $(Cu_{0.6}Ni_{0.4})_6Sn_5$ and $(Ni_{0.8}Cu_{0.2})_3Sn_4$. [19,20] The 1st term in the right-hand side of eq. (1) describes the number of Cu atoms in the solder before a reaction, while the 2nd term does the number of Cu atoms consumed for IMC formation.

After the 1st 1min reflow, from equation (1), the Cu content changes from 0.5 to 0.37 wt.% so that $(Ni,Cu)_3Sn_4$ is expected to form at the top joint during the 2nd reflow. During the 2nd 1min reflow, Cu is consumed at both solder joints and is estimated to decrease to 0.18wt.%. This value is close to the transition point of 0.2wt.%, from $(Cu,Ni)_6Sn_5$ to $(Ni,Cu)_3Sn_4$ formation as reported in ref. 13. Therefore, the transition is expected to occur at the end of the 2nd 1min reflow. Based on the estimation on Cu concentration, the MC phases observed in this study are consistent with the previous reports. [19,20]

2) Correlation between IMC spalling and brittle fracture

After lap-shear testing, the fracture surfaces were closely examined to analyze the fracture mode. Only two fracture modes were found ; ductile fracture through the bulk solder or brittle fracture through the interface between Ni_3Sn_4 and the Ni(P) film. Plane-view SEM micrographs of the ductile-fracture and the brittle-fracture solder joints are presented in Fig. 3(a) to (d). The white compounds on the pad in Fig. 3(d) are remaining Ni_3Sn_4 after the brittle fracture. Most Ni_3Sn_4 IMCs were found inside solder ball. In case of the brittle fracture, the surfaces of both ball and pad side were completely covered with tiny particles as shown in Fig. 3(e). The nano-particles were confirmed as Ni_3SnP grains by comparing the size and analyzing the composition with EDX (inset of Fig 3(b) ; Ni 55.34, P 22.17, and Sn 22.49 at.%). EDX analysis was performed at a low power of 10kV to minimize the penetration depth of X-ray. For a reference, a plane-view of the Ni_3SnP layer on a Ni(13P) film is presented in Fig. 3(f).

Table Ⅰ. Correlation between IMC spalling and the brittle fracture of ENIG/Pb-free solder interconnection.

solder	interface	reflow (min)	IMC	spalling area (%)	B-F area (%)
Sn-3.5Ag	top	1	Ni_3Sn_4	0	0
	bottom	2	Ni_3Sn_4	5.9	9.3
	top	5	Ni_3Sn_4	3.3	3.1
	bottom	6	Ni_3Sn_4	17.8	7.6
Sn-3.0Ag-0.5Cu	top	1	$(Ni,Cu)_3Sn_4$	0	0
	bottom	2	$(Cu,Ni)_6Sn_5$	0	0
	top	5	$(Ni,Cu)_3Sn_4$	0	0
	bottom	6	$(Cu,Ni)_6Sn_5$ $(Ni,Cu)_3Sn_4$	0	0

• B-F area denotes brittle-fractured area.

The results show that the Ni_3SnP layer is mechanically weak and the brittle fracture occurs through the Ni_3SnP layer. Since Kirkendall voids were found inside the Ni_3SnP layer [12,17], the brittle fracture might occur through the void areas in the Ni_3SnP phase. The brittle fracture was only found in Sn-3.5Ag solder joints where Ni_3Sn_4 IMCs spalled off. The spalling area and the brittle-fractured area were measured as a fraction of the fractured surface and summarized in Table Ⅰ. The brittle-fracture area does not match directly with the spalling area, which is not understood at present and needs further investigation. However, the experimental results provide an important implication that control of IMC spalling is crucial to ensure the reliability of ENIG/solder system since the Ni_3SnP layer grows during/after the spalling process [12].

3) Effect of intermediate layer deposition on IMC spalling

A thin intermediate layer of Sn or Cu was deposited on the Ni(9P) film by electroplating (EP) or electroless plating (EL).[22] And then, the Ni(9P) films with or without the intermediate layer were reacted with 130μm thick Sn-3.5Ag (solder paste) at 250°C up to 30min as depicted in Fig. 1(c). The thicknesses of the intermediated layers and the characteristics of the IMCs formed during the reactions were summarized in Table Ⅱ.

The Ni(9P)/electroplated (EP) Sn UBM successfully stopped Ni_3Sn_4 spalling up to 30min reaction, while the IMCs spalled off the Ni(9P) film without an intermediate layer only after 2min reaction as shown in Fig. 4(a) to (d). Though electroplating of Sn film didn't change the phase and composition of the IMC, it protected the surface of Ni(P) film and provided a good wettable surface during reflow reaction. On the other hand, the deposition of a thin Cu layer on the Ni(P) film altered the chemical structure of the IMCs in addition to the protection of the initial Ni(P) surface. For the solder joints with a Cu intermediate layer, ternary IMCs such

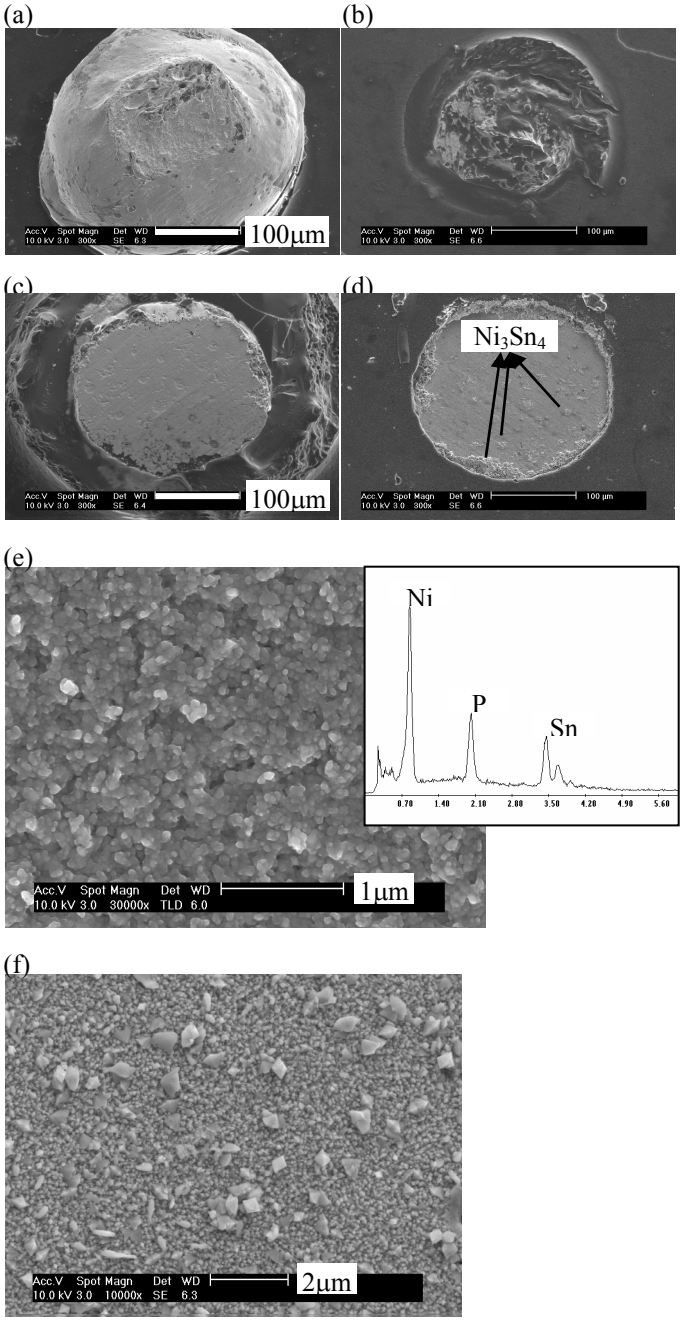

Fig. 3. Plane-view SEM micrographs showing (a) ball side and (b) pad side of typical ductile-fractured solder joint, (c) ball side and (d) pad side of typical brittle fractured solder joint, (e) magnified view of the brittle-fractured surface of (d) and composition analysis by EDX area scan at 10Kv, and (f) the Ni-Sn-P layer formed on the Ni(13P) film after Ni_3Sn_4 spalling (the solder was selectively etched away).

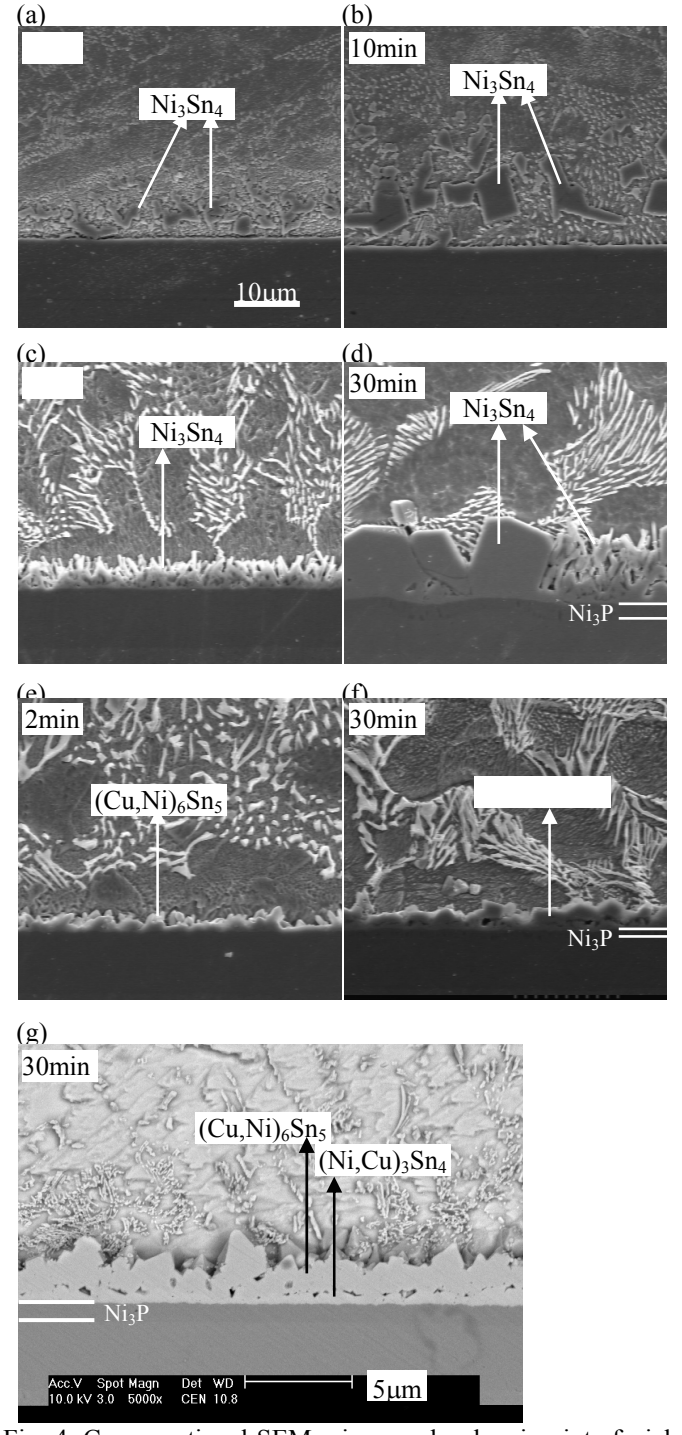

Fig. 4. Cross-sectional SEM micrographs showing interfacial microstructures after the reactions between 130μm thick Sn-3.5Ag (solder paste) and different UBMs at 250°C. ;
(a), (b) : Ni(9P) UBM after 2min and 10min reflow
(c), (d) : Ni(9P)/EP Sn (2μm) after 2min and 30min reflow
(e), (f) : Ni(9P)/EP Cu (0.9μm) after 2min and 30min reflow
(g) : Ni(9P)/EL Cu (0.7μm) after 30min reflow
- all the pictures except (g) are in same magnification.

as $(Ni,Cu)_3Sn_4$ and $(Cu,Ni)_6Sn_5$ was formed at the interface instead of Ni_3Sn_4 IMC. The Ni_3Sn_4 formed as needle-shape and changed into chunks with reaction time, while the ternary

Table Ⅱ. Characterization of the intermediate layers and interfacial IMCs formed during the reactions with Sn-3.5Ag solder.

inter-mediate layer	layer thickness (μm)	Cu wt.% before reaction	IMC phase and thickness (μm) after 30min reaction		Cu wt.% after reaction
EP Sn	2.0	-	Ni_3Sn_4	9.3	-
EP Cu	0.4	0.37	$(Ni,Cu)_3Sn_4$	3.8	0.17
EL Cu	0.7	0.64	$(Cu,Ni)_6Sn_5$	1.2	0.40*
			$(Ni,Cu)_3Sn_4$	0.5	
EP Cu	0.9	0.82	$(Cu,Ni)_6Sn_5$	3.2	0.18

* Cu wt.% after a formation of $(Cu,Ni)_6Sn_5$ IMC without considering $(Ni,Cu)_3Sn_4$ IMC.

IMCs was formed as a layer structure which effectively reduced the consumption of the Ni(P) film as a good diffusion barrier. As a result, the growth of the Ni_3P layer underneath thin ternary IMCs was under control as shown in Fig. 4(d), (f), and (g). All the intermediate layers deposited on the Ni(9P) film succeeded in preventing IMC spalling until 30min reaction at 250°C.

Assuming complete dissolution of the Cu layers into the solder, the intermediate Cu films can be converted to Cu wt.% comprising a Sn-3.5Ag-xCu solder. The dissolution of 0.4, 0.7, and 0.9 μm thick Cu layer will account for 0.37, 0.64, and 0.82 wt.% Cu in the Sn-3.5Ag-xCu solder as summarized in Table Ⅱ. A solubility limit of Cu in Sn-3.5Ag was reported to be 1.54wt.% at 260°C. [23] During the reaction with Ni(P)/EP Cu (0.4μm) UBM, only $(Ni,Cu)_3Sn_4$ IMC was formed from 2min to 30min reaction since the Cu content was less than 0.4wt.%. When the Cu concentration was more than 0.5wt.%, for 0.7 or 0.9μm thick Cu film, the $(Cu,Ni)_6Sn_5$ IMC was formed as reported in literatures.[19,20] After 30min reaction with Ni(P)/EP Cu (0.9μm) UBM, 3.2μm thick $(Cu,Ni)_6Sn_5$ IMC was formed and the Cu concentration decreased to 0.18wt.% close to the transition point of 0.2wt.%. [13] The change of Cu concentration in the solder was calculated with the measured thickness of the IMC using eq. (1). We confirmed that some $(Ni,Cu)_3Sn_4$ IMC was indeed formed underneath the $(Cu,Ni)_6Sn_5$ IMC in some areas of the specimen. However, after 30min reaction with Ni(P)/EL Cu (0.7μm) UBM, the Cu concentration in the solder was not estimated to decrease to 0.2 wt.% based on the calculation using the thickness of the $(Cu,Ni)_6Sn_5$ IMC even though a continuous $(Ni,Cu)_3Sn_4$ layer was clearly present as shown in Fig 4(g). Since the calculated Cu concentration in the solder after the formation of $(Cu,Ni)_6Sn_5$ was 0.4wt.%, we still need 0.2wt.% more consumption of Cu to reach the transition point (0.2wt.%). Large-grown $(Cu,Ni)_6Sn_5$ chunks were found inside the solder near the interface after the reactions with Ni(P)/EL Cu, while not found with Ni(P)/EP Cu. The $(Cu,Ni)_6Sn_5$ chunks inside the solder might account for 0.2wt.% more Cu consumption needed to reach the transition point. It is not obvious at present why the $(Cu,Ni)_6Sn_5$ IMC was found both in the solder and at the interface in the electroless plated Cu samples, while in the electroplated Cu samples most IMC were found only at the interface.

Conclusions

Correlation between IMC spalling and the brittle fracture of ENIG/solder joint has been studied by performing lap shear testing of PCBs having the Ni(P) metallization joined to Pb-free solders. Following conclusions are drawn in this study ;

(1) Ni_3Sn_4 IMC was formed and spalled off the Ni(P) surface in the solder joints made of Sn-3.5Ag, while Cu-Ni-Sn ternary IMCs were formed in Sn-3.0Ag-0.5Cu solder joints and didn't spalled off.

(2) The brittle fracture occurred through the Ni_3SnP layer in the Sn-3.5Ag solder pads where Ni_3Sn_4 IMC spalled. Control of IMC spalling is important to prevent the brittle fracture of ENIG/solder interconnection since the Ni_3SnP layer grows during/after the spalling process.

(3) A thin intermediate layer of Sn or Cu deposited on the Ni(P) film significantly suppressed IMC spalling. . The Sn layer provided protection of the Ni(P) surface and good wettable surface during reflow. The Cu film changed the chemical structure of the interfacial IMCs in addition to providing a good wettable surface.

(4) The Cu intermediate layer is considered as a better diffusion barrier since it effectively reduced a consumption of the Ni(P) film with the formation of layer-type Cu-Ni-Sn ternary IMCs.

Acknowledgments

This work was supported by the Center for Electronic Packaging Materials (CEPM) of Korea Science and Engineering Foundation.

References

1. T. I. Eijim, D. B. Hollesen, A. Holliday, S. A. Gahr, R. J. Coyle, "Assembly and reliability of thermaly enhanced high I/O BGA packages" *Proc 21st IEEE International Electronics manufacturing Symposium*, pp.25 (1997).
2. Z. Mei, M. Kauffmann, A. Eslambolchi, P. Johnson, "Brittle interfacial fracture of PBGA packages on electroless Ni/immersion Au" *Proc 48th Electronic Component and Technology Conference*, pp.952 (1998).
3. N. Biunno, "A root cause failure mechanism for solder joint integrity of electroless Ni/immersion gold surface finishes" *Proc IPC Printed Circuits Expo 1999*, s18-5 (1999).
4. G. M. Wenger, R. J. Coyle, P. P. Solan, J. K. Dorey, C. V. Dodd, R. Erich and A. Primavera, "Case sudies of brittle interfacial fractures in area array solder interconnects" *Proc 26th International Symposium for testing and failure analysis*, pp.355 (2000).
5. D. Cullen, E. Huenger, M. Toben, B. Houghton and K. Johal, "A study on interfacial fracture phenomenon of solder joints formed using the electroless

nickel/immersion gold surface finish" *Proc IPC works 2000*, s03-2 (2000).

6. C. H. Zhong and S. Yi, "Solder joint reliability of plastic ball grid array" *Soldering and Surface Mount Technology*, Vol.11, No.1 (1999), pp.44.
7. D. Goyal, T. Lane, P. Kinzie, C. Panichas, K. M. Chong and O. Villalobos, "Failure mechanism of brittle solder joint fracture in the presence of electroless Ni immersion gold (ENIG) interface" *Proc 52nd Electronic Component and Technology Conference*, pp.732 (2002).
8. S. Wiegele, P. Thompson, R. Lee and E. Ramsland, "Reliability and process characterization of electroless nickel-gold/solder flip chip interconnect technology" *Proc 48th Electronic Component and Technology Conference*, pp.861 (1998).
9. J. W. Jang, D. R. Frear, T. Y. Lee and K. N. Tu, "Morphology of interfacial reaction between lead-free solders and electroless Ni-P uner bump metallization" *J. Appl. Phys.*, Vol.88, No.11 (2000), pp.6359-6363.
10. Glenn O. Mallory and Juan B. Hadju, Electroless plating : fundamentals and applications, American electroplater and surface finishers society, Ch. 4 (1990).
11. R. Aschenbrenner, A. Ostmann, U. Beutler, J. Simon and H. Reichl, "Electroless nickel/copper plating as a new bump metallization" *IEEE Trans. CPMT, Part B*, Vol.18, No.2 (1995), pp.334-338.
12. Y. C. Sohn, Jin Yu, S. K. Kang, D. Y. Shih and T. Y. Lee, "Spalling of intermetallic compounds during the reaction between lead-free solders and electroless Ni-P metallization" *J. Mater. Res.*, Vol.19, No.8 (2004), pp. 2428-2436.
13. M. O. Alam, Y. C. Chan and K. N. Tu, "Effect of 0.5 wt% Cu in Sn-3.5%Ag solder on the interfacial reaction with Au/Ni metallization" *Chem. Mater.*, Vol.15, No.23 (2003), pp.4340-4342.
14. S. J. Wang and C. Y. Liu, "Retarding growth of Ni3P crystalline layer in Ni(P) substrate by reacting with Cu-bearing Sn(Cu) solders", *Scripta Mater.*, Vol.49, (2003), pp.813-818.
15. J. W. Jang, P. G. Kim, K. N. Tu, D. R. Frear and P. Thompson, "Solder reaction-assisted crystallization of electroless Ni-P under bump metallization in low cost flip chip technology" *J. Appl. Phys.*, Vol.85, No.12 (1999), pp.8456-8463.
16. Y. C. Sohn, Jin Yu, S. K. Kang, W. K. Choi and D. Y. Shih, "Study of the reaction mechanism between electroless Ni-P and Sn and its effect on the crystallization of Ni-P" *J. Mater. Res.*, Vol.18, No.1 (2003), pp.4-7.
17. K. Zeng, K. N. Tu, "Six cases of reliability study of Pb-free solder joints in electronic packaging technology" *Mater. Sci. and Eng. R.*, Vol.38, (2002), pp.55-105.
18. C. W. Hwang, K. Suganuma, M. Kiso and S. Hashimoto, "Interface microstructures between Ni-P alloy plating and Sn-Ag(-Cu) lead-free solders" *J. Mater. Res.*, Vol.18, No.11 (2003), pp. 2540-2543.
19. C. E. Ho, Y. L. Lin and C. R. Kao, "Strong effect of Cu concentration on the reaction between lead-free microelectronic solders and Ni" *Chem. Mater.*, Vol.14, No.3 (2002), pp.949-951.
20. C. E. Ho, R. Y. Tsai, Y. L. Lin and C. R. Kao, "Effect of Cu concentration on the reactions between Sn-Ag-Cu solders and Ni" *J. Electron. Mater.*, Vol.31, No.6 (2002), pp.584-590.
21. T. Siewart, S. Liu, D. R. Smith and J. C. Madeni, "Properties of Lead-free Solders, Release 4.0" National Institute of Standards and Technology & Colorado School of Mines (2002).
22. S. K. Kang, D. Y. Shih and Y. C. Sohn, YOR9-2003-0273-US1, US patent filed, July 30, 2004.
23. M. E. Loomans and M. E. Fine, "Tin-Silver-Copper eutectic temperature and composition" *Metall. Mater. Trans. A*, Vol.31A, No.4 (2000), pp.1155-1162.